History of desert dust deposition recorded in the Elbrus ice core.

Stanislav Kutuzov[1], Michel Legrand[2,3], Suzanne Preunkert[2,3], Patrick Ginot[2,3,6], Vladimir Mikhalenko[1], Karim Shukurov[4], Alexey Poliukhov[5], Pavel Toropov[1,5]

[1] Institute of Geography, Russian Academy of Sciences, Moscow, 119017, Russia
[2] Université Grenoble Alpes, CNRS, Institut des Géosciences de l'Environnement (IGE), Grenoble, 38402, France
[3] CNRS, Institut des Géosciences de l'Environnement (IGE), Grenoble, 38402, France
[4] A.M. Obukhov Institute of Atmospheric Physics of Russian Academy of Sciences, Moscow, 119017, Russia
[5] Faculty of Geography, Lomonosov Moscow State University, Moscow, 119991, Russia
[6] Observatoire des Sciences de l'Univers de Grenoble, IRD/UGA/CNRS, Grenoble, 38400, France

Correspondence to: Stanislav Kutuzov (kutuzov@igras.ru)

Abstract. Ice cores are one of the most valuable paleoarchives. Records from ice cores provide information not only about the amount of dust in the atmosphere but also about dust sources and their changes in the past. A 182 m long ice core was recovered from the western plateau of Mt. Elbrus (5115 m.a.s.l.) in 2009. This record was extended with a shallow ice core drilling in 2013. Here we analyse Ca^{2+} concentrations, a commonly used proxy of dust, recorded in the Elbrus ice core over the time period of 1774-2013 CE. The Ca^{2+} record reveals a quasi-decadal variability with a generally increasing trend. Using multiple regression analysis, we found a statistically significant spatial correlation of the Elbrus Ca^{2+} summer concentrations with precipitation and soil moisture content in the Levant region (specifically Syria and Iraq). The Ca^{2+} record also correlates with drought indices in North Africa (r=0.69 p<0.001) and Middle East regions (r=0.71 p<0.001). Dust concentrations prominently increase in the ice core over the past 200 years confirming that the recent droughts in the Fertile Crescent between 1998-2012 CE were the most severe aridity for at least the past two centuries. For the most recent 33 years (1979-2012 CE), significant correlations between Ca^{2+} and Pacific circulation indices (PDO, SOI and Niño 4) may indicate that the increased frequency of extreme El Niño and La Niña events due to a warming climate extended their influence to the Middle East.

1 Introduction

Dust is the most important aerosol emitted to the atmosphere by mass (Knippertz & Stuut, 2014). Atmospheric dust affects planetary radiation balance, atmospheric chemistry, biosphere and human health (Middleton, 2017). Despite the significance of atmospheric dust, knowledge of its regional variability and long term trends over past centuries is still poor (Mahowald et al., 2010). Dust concentration in the atmosphere depends on specific meteorological conditions, which may also be influenced by large scale circulation patterns (e.g. ENSO, NAO). Long term trends are controlled by changes in precipitation and vegetation cover in dust source regions, with the vegetation cover being dependent on both natural (climatic changes)

and anthropogenic (land cover change) causes. The complexity of dust emission, atmospheric transport and deposition mechanisms result in large uncertainties in atmospheric dust models (Mahowald et al., 2007). The discrepancies between models are partly explained by very limited observations of dust variability over the past. However, reliable information on multiannual dust variability back to 1980 is now available from satellite data.

5 Analysis of recent aerosol variations and trends over different land and ocean regions show that despite significant trends over some major continental source regions, average values demonstrate little change in the past three decades (1980-2009) because opposite trends cancel each other out in the global average (e.g. Chin et al., 2014). Recent broad-scale assessments of changes of dust emissions based on sedimentary achieves show that global dust emissions doubled since the mid‑18th century which was attributed to anthropogenic land use and short term climate variability (Hooper & Marx, 2018). Climate-

10 aerosol model simulations with the ability to separate natural and anthropogenic dust sources show that there was a 25% increase in dust emissions between the 19th century and today. These changes are attributed to climate change (56%) and anthropogenic land cover change (40%) although the model underestimates dust concentrations in Asia, Middle East, and the US (Stanelle et al., 2014).

Records of past changes in dust concentrations are essential to better constrain connections between dust emissions and both

15 natural and anthropogenic environmental changes. In this respect, proxy data is vital. Ice cores are natural archives of past concentrations of various impurities present in the atmosphere, including dust (e.g. Legrand & Mayewski, 1997). The particle concentrations in ice cores provide information not only on the concentrations of atmospheric dust in the past but also give insight into the strengths of the dust sources and their changes through the time. Polar ice cores from Greenland and Antarctica reconstruct the changes of dust content in the atmosphere over hundreds thousands of years at a

20 hemispherical scale (e.g., De Angelis et al., 1997; Delmonte et al., 2002; Legrand, 1987; Petit et al., 1999; Ruth et al., 2003). In contrast, data from ice cores drilled at mid-latitude mountain glaciers proximal to arid areas reconstruct local- to regional-scale dust aerosol emission histories over shorter timescales (e.g. Grigholm et al., 2015, 2017; Kaspari et al., 2009; Osterberg et al., 2008; Thompson, 2000; Bohleber et al., 2018).

Mineral dust from North Africa and deserts of the Middle East is regularly deposited on glaciers in the Caucasus Mountains

25 (Kutuzov et al., 2013; Kutuzov et al., 2015). Due to its high elevation (over 5000 m.a.s.l.) and proximity to arid and semi-arid areas, the Caucasus are a natural trap for desert dust. Conditions near the summit of Elbrus ensure the preservation of a reasonably long climatic record in an ice core not affected by melt water infiltration. High accumulation rates assure high temporal resolution of the ice-core data (Mikhalenko et al., 2015). In addition to a study focusing on the long-term trend of black carbon in the Elbrus ice (Lim et al., 2017), several studies of other chemical species are currently in progress,

30 including studies of calcium and of sulfate. Data are discussed in two companion papers including the glaciochemistry of the deep Elbrus ice core drilled in 2009 (Preunkert et al., this issue). Here, we report changes in Ca^{2+} concentrations recorded in the Elbrus ice core between 1774-2012 CE and connections with natural variability, climatic and land use changes in the dust source regions.

2. Location, climatology, and backward air-mass trajectories

The Caucasus are situated between the Black and Caspian seas, and generally trend east–southeast, with the Greater Caucasus range often considered as the divide between Europe and Asia. The 2020 glaciers in the Caucasus cover an area of 1193 ± 27 km^2 (Tielidze & Wheate, 2018). Elbrus mountain glaciers contain about 10% of Caucasus ice volume and cover an area of 112.6 km^2 (Kutuzov, et al., 2015) (Fig. 1). Glaciers cover an altitudinal range from 2800 to 5642 m a.s.l. with the coldest conditions present above 5200 m a.s.l. where mean summer air temperature stays below 0°C.

To characterize possible sources of aerosols deposited on glaciers, we calculated three-dimensional backward trajectories of air parcels (elementary air particles) arriving at the Elbrus plateau (5100 m a.s.l.) using the NOAA HYSPLIT_4 trajectory model (Draxler & Hess, 1998; Stein et al., 2015) and NCEP/NCAR Reanalysis data on 2.5°×2.5° grids (Kistler et al., 2001) for the 1948-2013 period. 10 day backward trajectories were calculated for every 6 hours for the whole period , resulting in a total of ~100k modelled backward trajectories. Over this time period, aerosol transport is defined by the westerlies. Elbrus glaciers receive aerosols from sources located in Turkey and the Mediterranean, Eastern and Central Europe, the Middle East, North Africa and Southern Russia (Fig. 1b).

To identify potential dust source contributions we also analysed vertical distribution of the backward trajectories. An objective criterion was chosen to extract locations of possible dust entrainment along the trajectories. The criterion is met when the air parcel is close to the ground, i.e. within the well-mixed boundary layer, allowing the uptake of mineral aerosols (Sodemann et al., 2006). Density plots using NCEP/NCAR Reanalysis data were calculated for 10 day backward trajectories which fell within the boundary layer. The majority of the backward trajectories show a south-west origin with the highest frequency over the Middle East, eastern Mediterranean and North Africa in all seasons. In winter (December-February) air masses tend to come from more remote locations while summer (June-August) reveals possible transport from the Caspian Sea region and Southern Russia (Fig. 2).

3. Methodology

3.1. Ice core analysis

A 181.8 m long ice core was recovered at the western plateau of Elbrus, in the central Caucasus (5115 m asl) during August-September 2009. Drilling was performed in a dry borehole with a lightweight electromechanical drilling system. Borehole temperatures ranged from -17 °C to 10 m depth to -2.4 °C at 181 m (Mikhalenko et al., 2015). Ice cores were packed in insulated core boxes and shipped in a frozen state to the cold laboratory of the Institute des Géosciences de l'Environnement (IGE) in Grenoble, France for analyses. A total of 3724 samples were prepared from the surface (2009) down to 168.6 m of the Elbrus core. Cores were subsampled and decontaminated under a clean bench located in a cold room using the methodology described in (Preunkert & Legrand, 2013). Due to the glacier compression with depth, we applied a variable sampling resolution of 10 cm from 0 – 157 m, and then a sampling resolution of every 2 cm below 157 m depth. As a result

(Fig. 3), the temporal resolution remains relatively consistent throughout the core, with 12 samples per summer over the 1950-2010 CE time period to 14 samples each summer over the 1900-1950 CE time period. In addition, a 20.5 m long ice core was extracted in June 2013 at the same location to expand the existing record from 2009 to 2012. In total 515 samples of the firn core were analysed (85 samples per year).

5   We determined cations (Na^+, K^+, Mg^{2+}, Ca^{2+}, and NH_4^+) using a Dionex ICS-1000 chromatograph equipped with a CS12 separator column. For anions, a Dionex 600 equipped with an AS11 separator column was used with an eluent mixture of H_2O, NaOH at 2.5 and 100 mM, and CH_3OH. A gradient pump system allows the determination of inorganic species (Cl^-, NO_3^-, and SO_4^{2-}) as well as short-chain carboxylates (Legrand et al., 2013). For all investigated ions, ice decontamination blanks were insignificant compared to respective concentrations in the ice cores.

3.2. Dating the core

Seasonal ice-core stratigraphy of chemical parameters and ice-core dating based on annual layer counting of the deep Elbrus ice core is described in detail in (Mikhalenko et al., 2015). The seasonal oscillations of NH_4^+ and succinic acid allow dating the core with seasonal resolution. Based on the ammonium and succinic acid profiles, each annual layer was divided into two parts corresponding to snow deposition under winter conditions and spring-summer-autumn conditions (Legrand et al., 2013; Mikhalenko et al., 2015; Susanne Preunkert et al., 2000). The annual counting was confirmed with 1 year uncertainty over the last one hundred years by reference horizons from a tritium peak (1963) and the Katmai 1912 horizon (Mikhalenko et al., 2015). Though the annual counting becomes less straight forward prior to 1860, Mikhalenko et al. (2015) reported an ice age of 1825 at 156.6 m depth (i.e., 122.3 meter water equivalent, mwe). This time scale is consistent with the presence of a volcanic horizon at approximately 1833-1840 such as Coseguina (1835). More recently, Preunkert et al. (this issue) extended the annual counting down to 168.5 m depth (i.e., 131.6 mwe) using the ammonium and succinate records demonstrating that the seasonally-resolved record extends back to 1774.

For the 2013 ice core the succinic acid data were not available. We therefore used a combination of NH_4^+, BC and $\delta^{18}O$ profiles for annual counting and seasonal dissection. These results suggest that the 2013 firn core extends back to 2007, as confirmed by the similar patterns of NH_4^+, Ca^{2+} and $\delta^{18}O$ between the first 3.8 mwe of the 2009 core and the 7.2-10.7 mwe interval of the 2013 core (Lim et al., 2017).

3.3. Data presentation

The amount of dust in ice cores depends on many factors and corresponds to the presence of dust particles in the atmosphere. Primarily, dust emissions are influenced by the characteristics of the dust source (soil type, geomorphology, soil moisture) as well as by meteorological conditions (surface winds). Once dust clouds are uplifted to the mid troposphere their transport depends on the main circulation patterns. In mountainous areas with high snow accumulation, wet deposition defines annual and seasonal aerosol concentrations. During spring and summer the majority of air masses arrive to the Elbrus site from arid

areas with calcareous soils. We consider that all of the Ca^{2+} in the Elbrus ice core is of natural origin and therefore Ca^{2+} concentrations can be considered as a proxy for dust.

Using ammonium and succinate stratigraphy to separate the winter and summer seasons (Sect. 3.2), we determined half-year summer and winter means from 1774 to 2010 (Fig. 4). In Fig. 5, we report the seasonal cycle of calcium and ammonium averaged over two different periods of the 20th century (1900-1950 and 1950-2010). As discussed in the next section, calcium present in the Elbrus ice has two distinct origins: (1) sporadic arrival of desert dust plume events at the site and (2) "background" concentrations. Combining the Ca^{2+} and acidity records, Preunkert et al., (this issue) identified samples which are likely influenced by desert dust events (616 samples on a total of 2524 samples in summer, 67 samples on a total of 1150 samples in winter). For Fig. 4, 5, and 6, we report total calcium and "background" (also denoted $Ca^{2+}_{red.}$, see details in section 4.1) concentrations. The difference between Ca^{2+} and Ca^{2+}_{red} is related to dust concentration (denoted Ca^{2+}_{dust}). To discuss the long-term winter and summer trends of calcium in relation to past climatic conditions, we also reported both total concentrations and those calculated after removal of samples suspected to contain input from large dust deposition events ($Ca^{2+}_{red.}$ Values; Fig. 6).

4. Results and discussion

The total dust deposited at Mt. Elbrus may have three different natural components: (i) dust from local sources (nunataks, rock outcrops), (ii) sporadic arrival of large aeolian desert dust events and (iii) large scale background continuous terrigenous aerosol emissions. Apart from regions strongly impacted by sea-salt aerosols, the presence of calcium in aerosols in continental atmospheres is expected to mainly originate from exposed continental sediments. Even in polar regions (Antarctica or Greenland), calcium in ice mainly comes from dust, where only a small fraction is related to sea-salt emitted from the ocean (De Angelis et al., 1997; Legrand, 1987). Assuming that Na^+ present in the ELB melted ice samples is only related to sea-salt emissions, and considering the $[Na^+]/[Ca^{2+}]$ ratio of 0.038 in seawater, we find that only 1.0 ± 0.7 % in summer (1.40 ± 1.0 % in winter) of total Ca^{2+} may be attributable to sea-salt emissions. That percentage is clearly an upper limit since, in precipitation deposited at continental free tropospheric sites (e.g. Legrand, 2002), Na^+ is not only related to sea-salt due to the presence of leachable sodium in alumino-silicate particles but also Na^+ from halide evaporates present in the deserts.

The volcanic rocks of Elbrus near the drilling site do not contain calcite and we can therefore assume that Ca^{2+} present in the Elbrus ice archive information on past dust emissions, including continuous background emissions and large dust plumes reaching the site. In the following sections, we attempt to separate these two possible calcium sources.

4.1. Calcium concentrations during desert dust events and background conditions

Large dust plumes originating from the Middle East and less frequently from the Sahara reach the Caucasus (Kutuzov et al., 2013). As seen in the Alps, these events disturb the chemistry of snow deposits to create calcium-rich alkaline snow layers

(Wagenbach et al., 1996). Deposition of these plumes disturbs the concentrations of numerous chemical species in Alpine ice because either they were present in dust at the emission stage or, being acidic, they interacted with alkaline material during transport (Usher et al., 2003). In this work, as well as in Preunkert et al. (this issue) Elbrus samples are considered to be impacted by dust events if they contain more than 120 ppb of calcium and are also below the 25% quartile of a robust spline

5   through the calculated raw acidity profile. These selection criteria result in 616 dust-depostion summer samples (from a total of 2524) and 67 winter samples (from a total of 1150).

The mean concentration of Ca^{2+} was 145 ppb with a maximum of 5506 ppb. Most of the dust from long distance transport is deposited on Elbrus during warm periods. The average background summer Ca^{2+} concentration was 103 ppb compared to 44 ppb in winter layers. Most of the large dust deposition events also occurs during the warm season which further increases the

10   difference between summer (178 ppb) and winter (54 ppb) layers.

As seen in Fig. 6, most of long-term calcium trend is detected in summer with: (1) more frequent arrivals of large dust events after 1950 and (2) an increase of 100 ppb of the calcium background level after 1950. The maximum annual concentrations were found in 1999 and 2000 annual layers (980 and 850 ppb).There was a pronounced period of increased dust content in the 1960s with a following decrease in late 1970s. Exceptional peaks compared to the background occur during the

15   following years: 1802, 1957, 1863, 1917, 1933, 1963, 1984, 1989, 1999, 2000, 2008 and 2009.

4.2. Increasing frequency of desert dust events

Warm season layers contain an increase in Ca^{2+} throughout the entire investigated time period. The most pronounced increase in peak Ca^{2+} concentrations occurred after 1950s (Fig. 6). It is important to emphasize that this appearance of more frequent calcium peaks after 1950 compared to the preceding decades cannot be attributed to a decreasing time resolution of

20   the record with a smoothing of events with depth (Fig. 3). More specifically, the enhanced occurrence of summer calcium peaks between 1960 and 1970 compared 1950-1960 does not correspond to a significant decrease of the temporal resolution (from 9 samples over the 1960-1970 years compared to 11-12 samples over the 1950-1960 years).

As discussed by Preunkert et al. (this issue), the composition of dust events reaching Elbrus in the summer is consistent with what is found in atmospheric aerosols collected at Mediterranean sites during large dust events. For instance, the

25   $[Mg^{2+}]/[Ca^{2+}]$ ratio in Elbrus samples containing dust (0.035) is similar to those in atmospheric dust aerosols from the Sahara or Middle East. In recent decades (1950-2010), over which time period more dust events were detected in the Elbrus ice, a clear spring maximum of the dust fraction (in April) is observed (Fig. 5). These April dust peaks are consistent with the timing of the arrival of large dust plumes at the site (Kutuzov et al., 2013).

4.3. Enhanced background concentrations

30   Figure 6 demonstrates an increase in the calcium background concentrations after 1950. This increase may be influenced by human activities, such as coal combustion and cement production, thereby contributing to the background calcium trend detected in the Elbrus ice. Similar impacts of anthropogenic emissions on various species in natural dust emissions,

including calcium, was reported by (Kalderon-Asael et al., 2009) demonstrating that, under strong stratification in the lower atmosphere in Israel, part of the atmospheric calcium may be anthropogenic nature. At the scale of Europe, Lee and Pacyna (1999) estimated that 0.8 Tg of anthropogenic calcium are emitted per year, coal combustion contributing for 60% and cement for 30% of total. To date, these anthropogenic calcium emissions remain however one order of magnitude weaker

5   than dust calcium emissions from North-East Africa (12 Tg yr^{-1}) or West Asia (12.7 Tg yr^{-1}) (Zhang et al., 2015).

Particles emitted during both coal combustion and cement production are rich in calcium (calcite). We therefore may expect a weaker $[Mg^{2+}]/[Ca^{2+}]$ ratio in particles emitted by these anthropogenic processes compared to that in natural dust particles. Examination of Mg^{2+} and Ca^{2+} in Elbrus ice layers that not impacted by dust events helps to determine a possible contribution of anthropogenic activities to the increasing background calcium trend in Elbrus ice. As seen in Fig. 7, the

10   $[Mg^{2+}_{red.}]/[Ca^{2+}_{red.}]$ ratio in Elbrus summer ice is of 0.069 over the 1960-2010 compared to 0.126 over the 1774-1920. If we attribute this recent decrease of $[Mg^{2+}_{red.}]/[Ca^{2+}_{red.}]$ to a growing impact over the recent decades of calcium from cement (neglecting the presence of soluble magnesium in cement), the mean increase of $Mg^{2+}_{red.}$ level (10.8 ppb over the 1774-1920 years and 17.6 ppb over the 1960-2010 years) would lead to a $Ca^{2+}_{red.}$ increase of 55 ppb from 1774-1920 to 1960-2010. This value is half of the observed $Ca^{2+}_{red.}$ increase between the two time periods (71 ppb over 1774-1920 and 183 ppb over 1960-

15   2010). These calculations suggest that half of the observed increase of background calcium concentration after 1950 are attributable to anthropogenic activities. As seen in Fig. 8, even prior to 1950 the $[Mg^{2+}_{red.}]/[Ca^{2+}_{red.}]$ ratio sometimes dropped to values as low as 0.1 or less (around 1820, 1850, 1865, or 1908). Although the time period 1940-1950 has a low ratio (0.09) the calcium concentrations moderately increased (27 ppb; less than a third of the overall increase after 1950). Figure 8 suggests that a decrease in the $[Mg^{2+}_{red.}]/[Ca^{2+}_{red.}]$ ratio is not always associated with enhanced calcium levels but that

20   enhanced magnesium levels also lead to an enhancement of the $[Mg^{2+}_{red.}]/[Ca^{2+}_{red.}]$ ratio. For instance, over 1853-1861, a mean $[Mg^{2+}_{red.}]/[Ca^{2+}_{red.}]$ ratio of 0.22 occurs at the same time as a relatively high $Mg^{2+}_{red.}$ level (16 ppb instead of 10.8 ppb over the 1774-1920 time period).

Another indirect argument against a dominant contribution from the growing impact of cement use on the background calcium levels at Elbrus derives from an earlier study of calcium and aluminium at the Col du Dome site, Mont Blanc,

25   France (De Angelis & Gaudichet, 1991). The authors demonstrate that both the increase of the frequency of dust arrival in the 1980s and the background dust levels occurred without any coinciding decrease of the aluminium to calcium ratio. Given the low aluminium content of cement compared to desert dust, these observations suggest that the Col du Dome site is not significantly impacted by growing use of cement. We may expect that this impact is even weaker at the Elbrus site.

4.4. Climatic factors

30   Two major dust sources contribute mineral particles to the Elbrus glaciers, the Sahara and the Middle East. It was established that majority of the small scale dust sources in the Middle East are located in northern Mesopotamia (northern Syria – north-western Iraq) and the Syrian Desert (Kutuzov et al., 2013). The Levant is a major source of atmospheric dust (Middleton, 1986) with natural, anthropogenic and hydrological (intermittent streams and lakes) sources. The area between the Tigris and

the Euphrates in Iraq contains natural desert dust sources while the Neinava region in Iraq was recently identified as the most active dust source in the Middle East (Moridnejad et al., 2015). In the northern Sahara strong sporadic dust storms originating in the Libyan desert and the foothills of the Ahaggar Mountains in eastern Algeria may reach the Caucasus in the spring (Kutuzov et al., 2013).

5 In order to assess which factors drive the variations in dust content in the Elbrus ice core, we compared the dust concentrations with various climatic parameters in the potential dust sources. A statistically significant spatial correlation occurs between Ca^{2+} and precipitation as well as between soil moisture content in the Middle East (Fig. 9). Unlike in the Middle East, no spatial correlation was found between Ca^{2+} and the amount of precipitation in North Africa. It should be noted, however, that the observation network is very sparse in the arid areas and there are much larger uncertainties in

10 Global Precipitation Climatology Centre (GPCC) datasets in North Africa.

The Ca^{2+} record was also compared with drought indices in potential dust sources in the Middle East (32-37° N; 38-45° E) and in North Africa (20-35° N; 0-35° E) (Fig. 10). The Standardised Precipitation-Evapotranspiration Index (SPEI) was averaged over the regions of interest (Vicente-Serrano et al., 2010). Ca^{2+} significantly correlates with drought indices for both regions. The highest correlations were found for the SPEI 3 index which is determined by aridity over the three

15 previous months. The correlation coefficient for the Middle East is statistically significant (p<0.001) and reaches 0.71. The correlation remains significant after trend removal (r=0.48, p<0.001 for 1974-2012 and 0.63 (p<0.001) for 1970-2012) (Fig. 10). Periods of dryer conditions in the Middle East region coincide with the increased Ca^{2+} concentrations and vice versa. During the period of droughts in both regions, a greater amount of mineral particles are emitted into the atmosphere, and transported to Caucasus glaciers during the spring and summer. The general increasing trend in dust content corresponds to

20 negative trends in precipitation and increased dryness of the soil.

Ca^{2+} correlates significantly with the SPEI 3 drought index for the North African region (r=0.69 p<0.001) but most of the correlation is defined by similar tendencies in two series. Drier conditions at the dust source region correspond to a positive trend in dust concentrations in the Elbrus ice core. The correlation weakens for the full detrended series (r=0.30, p<0.05) and increases in the later period, reaching 0.51 (p<0.001) in 1970-2012. Large portions of the annual dust flux in Elbrus can be

25 deposited during a single strong deposition event. Such events are more often associated with dust transport from the Sahara (Kutuzov et al., 2013). Dust emitted from North Africa can also mix with with dust from Middle Eastern sources during transport (Shahgedanova et al., 2013).

As evident from the Elbrus ice core record, the frequency of dust events and total Ca^{2+} concentrations has increased, where the most notable trend occurs after the 1950s. This increase corresponds with the recent analysis of centennial climate

30 change trends in Africa which depict a significant northward expansion of the Saharan desert in the winter (Thomas & Nigam, 2018). The desert conditions are observed across larger territories in recent years and are associated with a slightly negative trend in winter precipitation and an increase in surface air temperatures. In coastal North Africa, dry conditions dominated and rainfall decreased since the 1980s (Nicholson et al., 2018). The number of days in the eastern Mediterranean increased over the period 1958–2006 (Ganor et al., 2010).

Two periods of maximum Ca^{2+} concentrations in the ice core correspond to the two most severe drought episodes in the Middle East since the1940s, and occur during 1998–2000 and 2007-2009 (Barlow et al., 2016). The significant precipitation decline (up to 70%) during these years is explained by the dominance of the high pressure systems over the eastern Mediterranean during the winter and spring months (Trigo et al., 2010).

5   Our findings are supported by an analysis of the frequency of droughts in Syria. For the period from 1961 to 2009, 25 years with droughts were observed, resulting in ~40% of the years classified as drought years. On average, droughts lasted 4.5 years, although in the 1970s a single drought lasted 10 years (Breisinger et al., 2011). A number of droughts lasting 2 or more years significantly impacted agricultural production and livestock in the north-east of the country, where a single drought in 1961 resulted in the loss of 80% of camels and 50 % of sheep. During the drought of 1998–2001, 329,000 people
10   of which 47,000 were nomadic families were forced to eliminate livestock numbers and experienced an acute shortage of food (De Châtel, 2014).

Dust emission is influenced by anthropogenic land use and changes in land cover which impact wind-driven soil erosion. The magnitude of such impacts is highly uncertain as both climatic and anthropogenic processes occur simultaneously (Webb & Pierre, 2018). Unsustainable agricultural practices, overgrazing, and deforestation may significantly increase the
15   area of the dust sources. It should be noted however that only around 5% of the land in North Africa and the Middle East is suitable for agriculture; the rest consists of pastures, forests, shrubs, urban zones, badlands, rocky areas, and deserts (Sivakumar & Stefanski, 2007).

4.4.1. Atmospheric circulation patterns

The general increase in dust concentrations in the Elbrus ice core are accompanied by a quasi-decadal variability. To identify
20   the possible factors which influence the dryness in the dust sources and dust transport to the Caucasus Mountains, we investigated the Ca^{2+} record in relation with various circulation indices. Correlations were calculated for periods of 30 years, using 5 years sliding windows. All series were detrended prior to analysis. The following indices were analyzed: PDO, SOI, AMO, NAO, TPI (IPO) Niño 3, Niño 3.4, Niño 4, Niño 1-2 (https://www.esrl.noaa.gov/psd/gcos_wgsp/Timeseries/).

For the 33 year time period (1979-2012), significant correlations exist between Ca^{2+} and PDO, SOI and Niño 4 in the
25   preceding winter period. A significant correlation (r=0.47 p<0.01) for the Niño 4 index also exists for Dec-June in 1948-2012. The relationship between dust concentrations and circulation indices of the Pacific Ocean is illustrated by the spatial correlation of Ca^{2+} with sea surface temperatures (Supplementary Fig. 1). 23 out of 47 years of high dust deposition recorded in Elbrus ice core coincide with negative Niño 4 phases in 1900-2012. After the 1950s 19 out of 23 years of increased dust concentration correspond to the negative Niño 4 and negative PDO (Fig. 11). No statistically significant correlation was
30   found between the dust in the Elbrus ice core and the NAO index. Ca^{2+} also correlates with the SOI index of the preceding autumn and winter (Nov-Jan) over the last 50 years. It is still unclear whether circulation in the Pacific played a significant role in the precipitation patterns in these dust source regions before the mid-20th century or not. The uncertainties in

reanalysis data in this period are large and therefore do not allow us to draw any conclusions about the stability of the revealed correlations in time.

The relationship of precipitation in the Middle East region to the different large-scale circulation patterns are summarized in a recent review of the droughts in the Middle East and Southwest Asia (Barlow et al., 2016 and references therin). The

5 precipitation and occurrence of droughts in the Middle East region may be influenced by several major climatic features such as the NAO, southwest Asian and Indian monsoon, global-scale variability associated with ENSO and state of the western Pacific which together determine the strength of the general atmospheric circulation (Barlow et al., 2016).

A significant negative correlation was found between atmospheric dust concentrations in Syria and the PDO in springtime during 2003–2015. It was shown that a positive geopotential height anomaly is formed over the Arabian Peninsula and North

10 Africa during the positive phases of PDO (Pu & Ginoux, 2016). A positive PDO is characterised by an increase of cyclonic activity over the northern Pacific and northern Atlantic which occurs together with the intensification of subtropical antyciclones. Despite an increase in geopotential height, the positive PDO increases the probability of moisture transport to North Africa and Middle Eastern regions in the spring (Dai, 2013; Pu & Ginoux, 2016). This moisture is due to increased advection from the Mediterranean Sea which causes deep convection due to unstable stratification in the lower troposphere.

15 The negative PDO phases on the other hand are associated with a negative geopotential height anomaly in the middle troposphere over the Mediterranean and the Middle East and cyclonic activity in the region. Low pressure anomalies over Europe, the Southern Arabian Peninsula and north-eastern to eastern Africa create favourable conditions for westerly winds from North Africa and increase the probability of dust transport to the Caucasus.

Studies of interannual decadal variability of dust activity in the Arabian peninsula and Fertile Crescent suggest that the

20 occurrence of severe droughts and increased dust emission were influenced by the La Niña phase amplified by the negative PDO (Notaro et al., 2015). There are still large uncertainties in such connections due the lack of long-term observations (Pu & Ginoux, 2016). The correlation between Pacific circulation indices and the amount of dust in the Elbrus ice core supports these previous findings and may indicate an increase in the frequency of extreme El Niño and La Niña events with climate warming (Cai et al., 2015) which can then influence circulation over the Pacific Ocean and extend to the Middle East.

25 Our results are also in line with previous conclusions about the possible influence of large circulation patterns on the aridity of the tropics. Dai, 2011 suggests that the El Niño-Southern Oscillation, tropical Atlantic SSTs, and Asian monsoons played a significant role in the increase in global aridity since the 1970s over Africa, southern Europe, East and South Asia, and eastern Australia while recent warming has increased atmospheric moisture demand contributing to the drying . It is expected that due to anthropogenic climate change the tropical belt may expand toward the poles, shift precipitation patterns,

30 and lead to increasing the territory affected by droughts (Seidel et al., 2008). Model studies show that under global warming the large-scale circulation systems (jet streams and storm tracks) may shift poleward (Mbengue & Schneider, 2017). The size and intensity of the Hadley cell and the associated shift of the subtropical anticyclone zone are likely to occur over the 21st century, which should primarily affect the precipitation regime in subtropical latitudes (Lu et al., 2007). An expansion of the

global tropics since 1979 by 1° to 3° latitude was identified in both hemispheres although the mechanisms behind this tropical expansion are still unclear (Lucas et al., 2014).

4.5. Comparison to other paleo records

The first record of dust deposition history in the Caucasus was obtained by F.F. Davitaya in 1962 (Davitaya, 1969). This work was based on sampling of the firn layers from a crevasse located at the Kazbek plateau (4600 m asl). Based on dust layer counting Davitaya estimated that sampled firn layers covered the period between 1793 and 1962. Dust concentrations clearly increased by a factor of 3 was observed since the late 1920's. This increase was attributed to various reasons including local dust influence due to glacier retreat, industry development, fires, World War II and volcanic activity. Despite our different methodology and location, we qualitatively determined a similar long-term dust trend in the Elbrus ice core record. The average Ca^{2+} concentration over the same periods increases by a factor of 2.5 from 88 ppb in 1793-1925 to 224 ppb in 1925-1962.

An overall increasing trend in dust content and Ca^{2+} exists in Colle Gnifetti (Alps) ice cores after 1870 (Thevenon et al., 2009). Unlike in the Elbrus Ca^{2+} records, no significant long-term trend over the past 300 years exists in the Alps (Bohleber et al., 2018). In Central Asia, negative trends in dust concentrations were found in ice cores in Tien Shan (Grigholm et al., 2017) and in Tibetan Plateau (Grigholm et al., 2015). After the 1950s, calcium concentrations and multiannual and decadal variability significantly decrease in both Central Asian regions due to changes in dust storm frequency in arid areas related to regional trends in reduced zonal wind strengths (Grigholm et al., 2015).

A review of the dust paleo records demonstrates that 16 of the 25 compiled sedimentary archives from across the globe depict a doubling in dust emissions over the past ~250 years which was attributed to the impact of anthropogenic activity in source regions (Hooper and Max, 2018). Previous estimates for the atmospheric dust variability also suggests that desert dust doubled during the 20th century with some exceptions (Mahowald et al., 2010). All of the existing regional and global estimates of atmospheric dust variations in the past have large uncertainties due to limited and unevenly distributed paleodata records, which is especially true for the important dust sources of the North Africa, East Asia and Middle East/Central Asia (Mahowald et al., 2010). Tree ring reconstructions of the June-August drought variability over the past 900 years in the Mediterranean revealed that 1998-2012 was the driest period in the Levant since the 12th century (Cook et al., 2016). Similarly, the latter half of the 20th century was found to be one of the driest in the last nine centuries in north-western Africa (Touchan et al., 2011).

Understanding variations in dust concentrations over the Caucasus leads to a better understanding of the climate change consequences and atmospheric circulation patterns in the dust source regions. Arid and semi-arid regions in North Africa and the Middle East are unstable under the recent climatic changes. Temperature and hydrological anomalies during the last millennium have led to large variations in human occupation and agricultural production, with precipitation variability as a key factor in the productivity in the Middle East region (Kaniewski, 2012). The Elbrus ice core record confirms previous

findings (Cook et al., 2016; Kelley et al., 2015) that the recent droughts in 1998- were the most severe over at least the past three centuries.

5. Conclusions

This paper presents the Ca^{2+} record from the Elbrus ice core and provides a valuable archive of regional atmospheric dust variability in the past. Ca^{2+} concentrations in the Elbrus ice core are a proxy for atmospheric dust transported over long distances from primary dust sources in North Africa and the Middle East. The Ca^{2+} record shows that recent decades were characterized by the highest dust emission activity since 1774. From the 1970s onward, Saharan dust deposition events significantly impact the dust deposition in the Caucasus where this deposition coincides with the dryer conditions. Ca^{2+} also significantly correlates spatially with precipitation and soil moisture content in the Middle East. The correlation between circulation indices and amount of dust in the Elbrus ice core indicate that the influence of circulation over the Pacific Ocean extended to the Middle East.

Data availability

Calcium data can be made available for scientific purposes upon request to the authors (contact: kutuzov@igras.ru; suzanne.Preunkert@univ-grenoble-alpes.fr or michel.legrand@univ-grenoble-alpes).

Author contributions

S. Kutuzov performed research, analyzed data and wrote the original manuscript. M. Legrand analyzed ice samples and data, and contributed to the original manuscript. S. Preunkert analyzed ice samples and commented original manuscript. P. Ginot and V.Mikhalenko performed analysis and commented original manuscript. K. Shukurov calculated backward trajectories commented original manuscript. A. Poliukhov and P. Toropov analyzed climatic data and atmospheric circulation patterns and commented original manuscript.

Acknowledgments

Research was supported by RSF grant 17-17-01270. The Les Enveloppes Fluides et l'Environnement- Chimie Atmosphérique (CNRS) program entitled "Evolution séculaire de la charge et composition de l'aérosol organique au dessus de l'Europe" provided funding for analysis in France, with the support of Agence de l'Environnement et de la Maîtrise de l'Energie. Backward trajectory analysis was supported by Presidium Program of the Russian Academy of Sciences No. 20. Interpretation of the shallow core was supported by the President Grants for Government Support of Young Russian Scientists and the Leading Scientific Schools of the Russian Federation grant № MK-2508.2017.5.

References

De Angelis, M. and Gaudichet, A.: Saharan dust deposition over Mont Blanc (French Alps) during the last 30 years, Tellus B, 43(1), 61–75, doi:10.1034/j.1600-0889.1991.00005.x, 1991.

5   De Angelis, M., Steffensen, J. P., Legrand, M., Clausen, H. and Hammer, C.: Primary aerosol (sea salt and soil dust) deposited in Greenland ice during the last climatic cycle: Comparison with east Antarctic records, J. Geophys. Res. Ocean., 102(C12), 26681–26698, doi:10.1029/97JC01298, 1997.

Barlow, M., Zaitchik, B., Paz, S., Black, E., Evans, J. and Hoell, A.: A review of drought in the Middle East and southwest Asia, J. Clim., 29(23), 8547–8574, doi:10.1175/JCLI-D-13-00692.1, 2016.

10   Bohleber, P., Erhardt, T., Spaulding, N., Hoffmann, H., Fischer, H. and Mayewski, P.: Temperature and mineral dust variability recorded in two low-accumulation Alpine ice cores over the last millennium, Clim. Past, 14(1), 21–37, doi:10.5194/cp-14-21-2018, 2018.

Breisinger, C., Zhu, T., Al Riffai, P., Nelson, G. C., Robertson, R., Funes, J. and Verner, D.: Global and Local Economic Impacts of Climate Change in Syria and Options for Adaptation, Food Policy, (June), 57 [online] Available from:
15   http://www.ifpri.org/publication/global-and-local-economic-impacts-climate-change-syria-and-options-adaptation, 2011.

Cai, W., Santoso, A., Wang, G., Yeh, S. W., An, S. Il, Cobb, K. M., Collins, M., Guilyardi, E., Jin, F. F., Kug, J. S., Lengaigne, M., Mcphaden, M. J., Takahashi, K., Timmermann, A., Vecchi, G., Watanabe, M. and Wu, L.: ENSO and greenhouse warming, Nat. Clim. Chang., 5(9), 849–859, doi:10.1038/nclimate2743, 2015.

De Châtel, F.: The Role of Drought and Climate Change in the Syrian Uprising: Untangling the Triggers of the Revolution,
20   Middle East. Stud., 50(4), 521–535, doi:10.1080/00263206.2013.850076, 2014.

Chin, M., Diehl, T., Tan, Q., Prospero, J. M., Kahn, R. A., Remer, L. A., Yu, H., Sayer, A. M., Bian, H., Geogdzhayev, I. V., Holben, B. N., Howell, S. G., Huebert, B. J., Hsu, N. C., Kim, D., Kucsera, T. L., Levy, R. C., Mishchenko, M. I., Pan, X., Quinn, P. K., Schuster, G. L., Streets, D. G., Strode, S. A. and Torres, O.: Multi-decadal aerosol variations from 1980 to 2009: A perspective from observations and a global model, Atmos. Chem. Phys., 14(7), 3657–3690, doi:10.5194/acp-14-
25   3657-2014, 2014.

Cook, B. I., Anchukaitis, K. J., Touchan, R., Meko, D. M. and Cook, E. R.: Spatiotemporal drought variability in the mediterranean over the last 900 years, J. Geophys. Res., 121(5), 2060–2074, doi:10.1002/2015JD023929, 2016.

Dai, A.: Drought under global warming: A review, Wiley Interdiscip. Rev. Clim. Chang., 2(1), 45–65, doi:10.1002/wcc.81, 2011.

30   Davitaya, F. F.: Atmospheric dust content as a factor affecting glaciation and climatic change, Ann. Assoc. Am. Geogr., 59(3), 552–560, doi:10.1111/j.1467-8306.1969.tb00690.x, 1969.

Delmonte, B., Petit, J.-R. and Maggi, V.: Glacial to Holocene implications of the new 27000-year dust record from the EPICA Dome C (East Antarctica) ice core, Clim. Dyn., 18(8), 647–660, doi:10.1007/s00382-001-0193-9, 2002.

Draxler, R. R. and Hess, G. D.: An overview of the HYSPLIT_4 modeling system of trajectories, dispersion, and deposition.,
35   Aust. Meteor. Mag., 47, 295–308, 1998.

Ganor, E., Osetinsky, I., Stupp, A. and Alpert, P.: Increasing trend of African dust, over 49 years, in the eastern Mediterranean, J. Geophys. Res. Atmos., 115(7), 1–7, doi:10.1029/2009JD012500, 2010.

Grigholm, B., Mayewski, P. A., Kang, S., Zhang, Y., Morgenstern, U., Schwikowski, M., Kaspari, S., Aizen, V., Aizen, E., Takeuchi, N., Maasch, K. A., Birkel, S., Handley, M. and Sneed, S.: Twentieth century dust lows and the weakening of the westerly winds over the Tibetan Plateau, Geophys. Res. Lett., 42(7), 2434–2441, doi:10.1002/2015GL063217, 2015.

5 Grigholm, B., Mayewski, P. A., Aizen, V., Kreutz, K., Aizen, E., Kang, S., Maasch, K. A. and Sneed, S. B.: A twentieth century major soluble ion record of dust and anthropogenic pollutants from Inilchek Glacier, Tien Shan, J. Geophys. Res., 122(3), 1884–1900, doi:10.1002/2016JD025407, 2017.

Hooper, J. and Marx, S.: A global doubling of dust emissions during the Anthropocene?, Glob. Planet. Change, 169(June), 70–91, doi:10.1016/j.gloplacha.2018.07.003, 2018.

Kalderon-Asael, B., Erel, Y., Sandler, A. and Dayan, U.: Mineralogical and chemical characterization of suspended
10 atmospheric particles over the east Mediterranean based on synoptic-scale circulation patterns, Atmos. Environ., 43(25), 3963–3970, doi:10.1016/j.atmosenv.2009.03.057, 2009.

Kaniewski, D.: Drought is a recurring challenge in the Middle East, Proc., doi:10.1073/pnas.1116304109/-/DCSupplemental.www.pnas.org/cgi/doi/10.1073/pnas.1116304109, 2012.

Kaspari, S., Mayewski, P. a., Handley, M., Kang, S., Hou, S., Sneed, S., Maasch, K. and Qin, D.: A High-Resolution Record
15 of Atmospheric Dust Composition and Variability since a.d. 1650 from a Mount Everest Ice Core, J. Clim., 22(14), 3910–3925, doi:10.1175/2009JCLI2518.1, 2009.

Kelley, C. P., Mohtadi, S., Cane, M. A., Seager, R. and Kushnir, Y.: Climate change in the Fertile Crescent and implications of the recent Syrian drought, Proc. Natl. Acad. Sci., 112(11), 3241–3246, doi:10.1073/pnas.1421533112, 2015.

Kistler, R., Collins, W., Saha, S., White, G., Woollen, J., Kalnay, E., Chelliah, M., Ebisuzaki, W., Kanamitsu, M., Kousky,
20 V., van den Dool, H., Jenne, R. and Fiorino, M.: The NCEP–NCAR 50–Year Reanalysis: Monthly Means CD–ROM and Documentation, Bull. Am. Meteorol. Soc., 82(2), 247–267, doi:10.1175/1520-0477(2001)082<0247:TNNYRM>2.3.CO;2, 2001.

Knippertz, P. and Stuut, J. B. W.: Mineral dust: A key player in the earth system, Miner. Dust A Key Play. Earth Syst., 1–509, doi:10.1007/978-94-017-8978-3, 2014.

25 Kutuzov, S., Shahgedanova, M., Mikhalenko, V., Lavrentiev, I. and Kemp, S.: Desert dust deposition on Mt. Elbrus, Caucasus Mountains, Russia in 2009–2012 as recorded in snow and shallow ice core: high-resolution "provenancing", transport patterns, physical properties and soluble ionic composition, Cryosph. Discuss., 7(2), 1621–1672, doi:10.5194/tcd-7-1621-2013, 2013a.

Kutuzov, S., Shahgedanova, M., Mikhalenko, V., Ginot, P., Lavrentiev, I. and Kemp, S.: High-resolution provenance of
30 desert dust deposited on Mt. Elbrus, Caucasus in 2009-2012 using snow pit and firn core records, Cryosph., 7(5), 1481–1498, doi:10.5194/tc-7-1481-2013, 2013b.

Kutuzov, S. S., Lavrentiev, I. I., Vasilenko, E. V., Macheret, Y. Y., Petrakov, D. A. and Popov, G. V.: Estimation of the greater caucasus glaciers volume, using radio-echo sounding data and modelling, Earth's Cryosph., 19(1), 78–88, 2015a.

Kutuzov, S. S., Mikhalenko, V. N., Shahgedanova, M. V., Ginot, P., Kozachek, A. V., Kuderina, T. M., Lavrentiev, I. I. and
35 Popov, G. V.: Ways of far-distance dust transport onto Caucasian glaciers and chemical composition of snow on the Western plateau of Elbrus, Ice Snow, 127(3), 5, doi:10.15356/2076-6734-2014-3-5-15, 2015b.

Lee, D. S. and Pacyna, J. M.: An industrial emissions inventory of calcium for Europe, Atmos. Environ., 33(11), 1687–1697, doi:10.1016/S1352-2310(98)00286-6, 1999.

Legrand, M.: Chemistry of Antarctic snow and ice, Le J. Phys. Colloq., 48(C1), C1-77-C1-86,
40 doi:10.1051/jphyscol:1987111, 1987.

Legrand, M.: Seasonally resolved Alpine and Greenland ice core records of anthropogenic HCl emissions over the 20th century, J. Geophys. Res., 107(D12), 4139, doi:10.1029/2001JD001165, 2002.

Legrand, M. and Mayewski, P.: Glaciochemistry of polar ice cores: A review, Rev. Geophys., 35(3), 219–243, doi:10.1029/96RG03527, 1997.

Legrand, M., Preunkert, S., May, B., Guilhermet, J., Hoffman, H. and Wagenbach, D.: Major 20th century changes of the content and chemical speciation of organic carbon archived in Alpine ice cores: Implications for the long-term change of
5 organic aerosol over Europe, J. Geophys. Res. Atmos., 118(9), 3879–3890, doi:10.1002/jgrd.50202, 2013.

Lim, S., Faïn, X., Ginot, P., Mikhalenko, V., Kutuzov, S., Paris, J. D., Kozachek, A. and Laj, P.: Black carbon variability since preindustrial times in the eastern part of Europe reconstructed from Mt. Elbrus, Caucasus, ice cores, Atmos. Chem. Phys., 17(5), doi:10.5194/acp-17-3489-2017, 2017.

Lu, J., Vecchi, G. A. and Reichler, T.: Expansion of the Hadley cell under global warming, Geophys. Res. Lett., 34(6),
10 L06805, doi:10.1029/2006GL028443, 2007.

Lucas, C., Timbal, B. and Nguyen, H.: The expanding tropics: a critical assessment of the observational and modeling studies, Wiley Interdiscip. Rev. Clim. Chang., 5(1), 89–112, doi:10.1002/wcc.251, 2014.

Mahowald, N. M., Ballantine, J. a., Feddema, J. and Ramankutty, N.: Global trends in visibility: implications for dust sources, Atmos. Chem. Phys. Discuss., 7(1), 3013–3071, doi:10.5194/acpd-7-3013-2007, 2007.

15 Mahowald, N. M., Kloster, S., Engelstaedter, S., Moore, J. K., Mukhopadhyay, S., McConnell, J. R., Albani, S., Doney, S. C., Bhattacharya, A., Curran, M. A. J., Flanner, M. G., Hoffman, F. M., Lawrence, D. M., Lindsay, K., Mayewski, P. A., Neff, J., Rothenberg, D., Thomas, E., Thornton, P. E. and Zender, C. S.: Observed 20th century desert dust variability: Impact on climateand biogeochemistry, Atmos. Chem. Phys., 10(22), 10875–10893, doi:10.5194/acp-10-10875-2010, 2010.

Mbengue, C. and Schneider, T.: Storm-Track Shifts under Climate Change: Toward a Mechanistic Understanding Using
20 Baroclinic Mean Available Potential Energy, J. Atmos. Sci., 74(1), 93–110, doi:10.1175/JAS-D-15-0267.1, 2017.

Middleton, N. J.: Desert dust hazards: A global review, Aeolian Res., 24, 53–63, doi:10.1016/j.aeolia.2016.12.001, 2017.

Mikhalenko, V., Sokratov, S., Kutuzov, S., Ginot, P., Legrand, M., Preunkert, S., Lavrentiev, I., Kozachek, A., Ekaykin, A., Fain, X., Lim, S., Schotterer, U., Lipenkov, V. and Toropov, P.: Investigation of a deep ice core from the Elbrus western plateau, the Caucasus, Russia, Cryosphere, 9(6), doi:10.5194/tc-9-2253-2015, 2015.

25 Moridnejad, A., Karimi, N. and Ariya, P. A.: A new inventory for Middle East dust source points, Environ. Monit. Assess., 187(9), 582, doi:10.1007/s10661-015-4806-x, 2015.

Nicholson, S. E., Funk, C. and Fink, A. H.: Rainfall over the African continent from the 19th through the 21st century, Glob. Planet. Change, 165(May 2017), 114–127, doi:10.1016/j.gloplacha.2017.12.014, 2018.

Notaro, M., Yu, Y. and Kalashnikova, O. V: Journal of Geophysical Research : Atmospheres, 229–249,
30 doi:10.1002/2015JD023855.Received, 2015.

Osterberg, E., Mayewski, P., Kreutz, K., Fisher, D., Handley, M., Sneed, S., Zdanowicz, C., Zheng, J., Demuth, M., Waskiewicz, M. and Bourgeois, J.: Ice core record of rising lead pollution in the North Pacific atmosphere, Geophys. Res. Lett., 35(5), L05810, doi:10.1029/2007GL032680, 2008.

Petit, J. R., Jouzel, J., Raynaud, D., Barkov, N. I., Barnola, J. M., Basile, I., Bender, M., Chappellaz, J., Davis, M., Delaygue,
35 G., Delmotte, M., Kotlyakov, V. M., Legrand, M., Lipenkov, V. Y., Lorius, C., Pépin, L., Ritz, C., Saltzman, E. and Stievenard, M.: Climate and atmospheric history of the past 420,000 years from the Vostok ice core, Antarctica, Nature, 399, 429–436, doi:10.1038/20859, 1999.

Preunkert, S. and Legrand, M.: Towards a quasi-complete reconstruction of past atmospheric aerosol load and composition (organic and inorganic) over Europe since 1920 inferred from Alpine ice cores, Clim. Past, 9(4), 1403–1416, doi:10.5194/cp-
40 9-1403-2013, 2013.

Preunkert, S., Wagenbach, D., Legrand, M. and Vincent, C.: Col du Dôme (Mt Blanc Massif, French Alps) suitability for ice-core studies in relation with past atmospheric chemistry over Europe, Tellus B Chem. Phys. Meteorol., 52(3), 993–1012, doi:10.3402/tellusb.v52i3.17081, 2000.

Pu, B. and Ginoux, P.: The impact of the Pacific Decadal Oscillation on springtime dust activity in Syria, Atmos. Chem.
5   Phys., 16(21), 13431–13448, doi:10.5194/acp-16-13431-2016, 2016.

Ruth, U., Wagenbach, D., Steffensen, J. P. and Bigler, M.: Continuous record of microparticle concentration and size distribution in the central Greenland NGRIP ice core during the last glacial period, J. Geophys. Res., 108(D3), 4098, doi:10.1029/2002JD002376, 2003.

Seidel, D. J., Fu, Q., Randel, W. J. and Reiohler, T. J.: Widening of the tropical belt in a changing climate, Nat. Methods,
10   1(1), 21–24, doi:10.1038/ngeo.2007.38, 2008.

Shahgedanova, M., Kutuzov, S., White, K. H. and Nosenko, G.: Using the significant dust deposition event on the glaciers of Mt.~Elbrus, Caucasus Mountains, Russia on 5 May 2009 to develop a method for dating and "provenancing" of desert dust events recorded in snow pack, Atmos. Chem. Phys., 13(4), 1797–1808, doi:10.5194/acp-13-1797-2013, 2013.

Sivakumar, M. V. K. and Stefanski, R.: Climate and Land Degradation --- an Overview, in Climate and Land Degradation,
15   edited by M. V. K. Sivakumar and N. Ndiang'ui, pp. 105–135, Springer Berlin Heidelberg, Berlin, Heidelberg., 2007.

Sodemann, H., Palmer, A. S., Schwierz, C., Schwikowski, M. and Wernli, H.: The transport history of two Saharan dust events archived in an Alpine ice core, Atmos. Chem. Phys., 6(3), 667–688, doi:10.5194/acp-6-667-2006, 2006.

Stanelle, T., Bey, I., Raddatz, T., Reick, C. and Tegen, I.: Journal of Geophysical Research : Atmospheres, 526–546, doi:10.1002/2014JD022062.Received, 2014.

20   Stein, A. F., Draxler, R. R., Rolph, G. D., Stunder, B. J. B., Cohen, M. D. and Ngan, F.: Noaa's Hysplit atmospheric transport and dispersion modeling system, Bull. Am. Meteorol. Soc., 96(12), 2059–2077, doi:10.1175/BAMS-D-14-00110.1, 2015.

Thevenon, F., Anselmetti, F. S., Bernasconi, S. M. and Schwikowski, M.: Mineral dust and elemental black carbon records from an Alpine ice core (Colle Gnifetti glacier) over the last millennium, J. Geophys. Res., 114(D17), D17102,
25   doi:10.1029/2008JD011490, 2009.

Thomas, N. and Nigam, S.: Twentieth-century climate change over Africa: Seasonal hydroclimate trends and sahara desert expansion, J. Clim., 31(9), 3349–3370, doi:10.1175/JCLI-D-17-0187.1, 2018.

Thompson, L. G.: A High-Resolution Millennial Record of the South Asian Monsoon from Himalayan Ice Cores, Science (80-.)., 289(5486), 1916–1919, doi:10.1126/science.289.5486.1916, 2000.

30   Tielidze, L. G. and Wheate, R. D.: The Greater Caucasus Glacier Inventory (Russia, Georgia and Azerbaijan), Cryosph., 12(1), 81–94, doi:10.5194/tc-12-81-2018, 2018.

Touchan, R., Anchukaitis, K. J., Meko, D. M., Sabir, M., Attalah, S. and Aloui, A.: Spatiotemporal drought variability in northwestern Africa over the last nine centuries, Clim. Dyn., 37(1–2), 237–252, doi:10.1007/s00382-010-0804-4, 2011.

Trigo, R. M., Gouveia, C. M. and Barriopedro, D.: The intense 2007-2009 drought in the Fertile Crescent: Impacts and
35   associated atmospheric circulation, Agric. For. Meteorol., 150(9), 1245–1257, doi:10.1016/j.agrformet.2010.05.006, 2010.

Usher, C. R., Michel, A. E. and Grassian, V. H.: Reactions on Mineral Dust, Chem. Rev., 103(12), 4883–4940, doi:10.1021/cr020657y, 2003.

Vicente-Serrano, S. M., Beguería, S. and López-Moreno, J. I.: A Multiscalar Drought Index Sensitive to Global Warming: The Standardized Precipitation Evapotranspiration Index, J. Clim., 23(7), 1696–1718, doi:10.1175/2009JCLI2909.1, 2010.

40   Wagenbach, D., Preunkert, S., Schäfer, J., Jung, W. and Tomadin, L.: Northward Transport of Saharan Dust Recorded in a Deep Alpine Ice Core, in The Impact of Desert Dust Across the Mediterranean, edited by S. Guerzoni and R. Chester, pp. 291–300, Springer Netherlands, Dordrecht., 1996.

Webb, N. P. and Pierre, C.: Quantifying Anthropogenic Dust Emissions, Earth's Futur., 6(2), 286–295, doi:10.1002/2017EF000766, 2018.

Zhang, Y., Mahowald, N., Scanza, R. A., Journet, E., Desboeufs, K., Albani, S., Kok, J. F., Zhuang, G., Chen, Y., Cohen, D. D., Paytan, A., Patey, M. D., Achterberg, E. P., Engelbrecht, J. P. and Fomba, K. W.: Modeling the global emission,
5 transport and deposition of trace elements associated with mineral dust, Biogeosciences, 12(19), 5771–5792, doi:10.5194/bg-12-5771-2015, 2015.

Table 1. Ca^{2+} concentrations in Elbrus ice cores in different periods including total concentrations and excluding background samples from the large dust deposition events.

	Ca^{2+} concentration (*ppb*)			
	summer (total)	summer (background)	winter (total)	winter (background)
1774-1800	65	64	42	42
1800-1850	78	69	52	46
1850-1900	100	69	43	36
1900-1950	156	83	37	33
1950-2000	344	181	75	58
2000-2012	439	212	99	64
1774-2012	172	103	54	44

5 **Table 2.** Correlation coefficient of the Elbrus Ca^{2+} data and large-scale atmospheric circulation indices.

	1948-2012	1979-2012
PDO (Dec-June)	-0.35	-0.42
SOI (Oct-Jan)	0.40	0.49
Niño 4 (Dec-June)	-0.47	-0.57
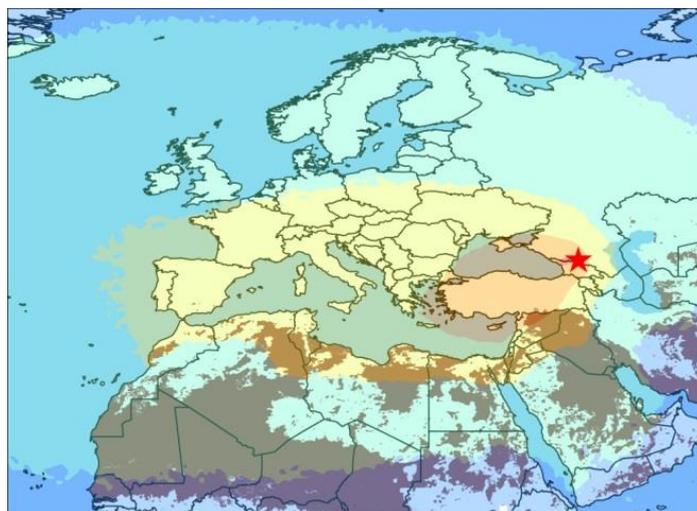
Figure 1: Location of Elbrus (red star) and dust sources (dark shading) based on (Ginoux et al., 2012). Annual NOAA HYSPLIT_4 10-day backward trajectory density plots for the period 1948-2013 using NCEP/NCAR Reanalysis. Trajectories were run every 6 hrs. Colours are the relative contributions of the source areas determined from 10-day backward trajectories in 0.5x0.5 degree grids.
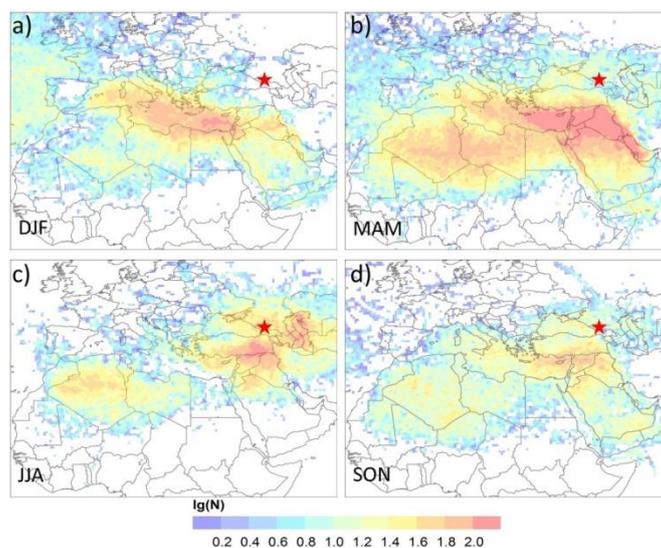
Figure 2: NOAA HYSPLIT_4 10-day backward trajectories density plots for the period 1948-2013 using NCEP/NCAR Reanalysis. Trajectories were run every 6 hrs. Only backward trajectories within the boundary layer were considered. Contribution of 10-day backward trajectories in 0.5x0.5 degree grids.
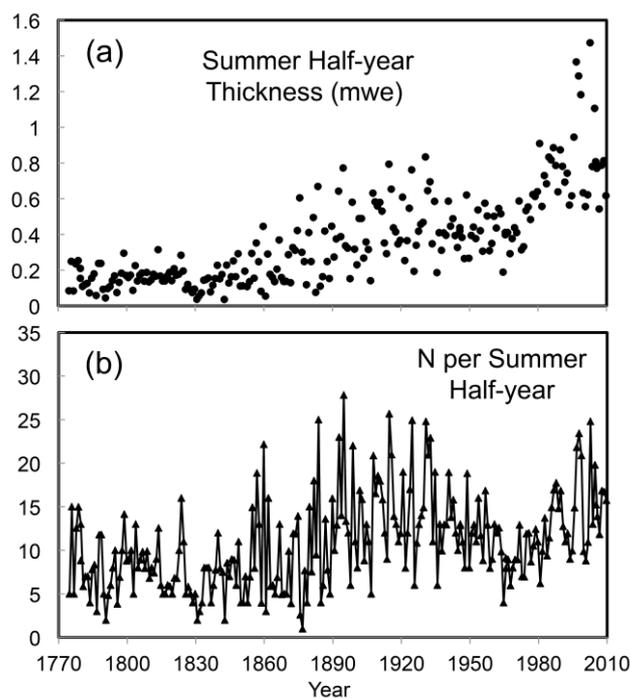
Figure 3: (a): Mean summer half-year thickness along the Elbrus deep ice core. (b): Numbers of samples (N) spanning summer half-years. See details in Preunkert et al., this issue.
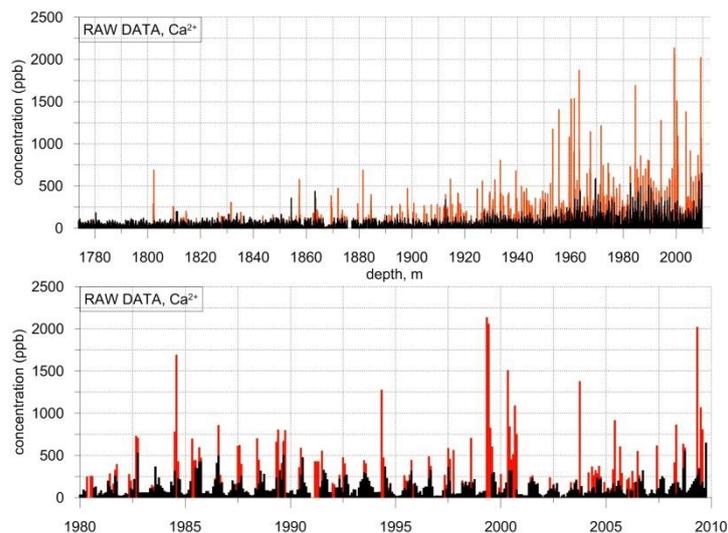
Figure 4: (a): Total (red) and background (after the removal of samples influenced by large dust deposition events, black) Ca^{2+} concentrations (ppb) in Elbrus ice core samples. The full record (a) and the upper section of the ice core (b) are shown.
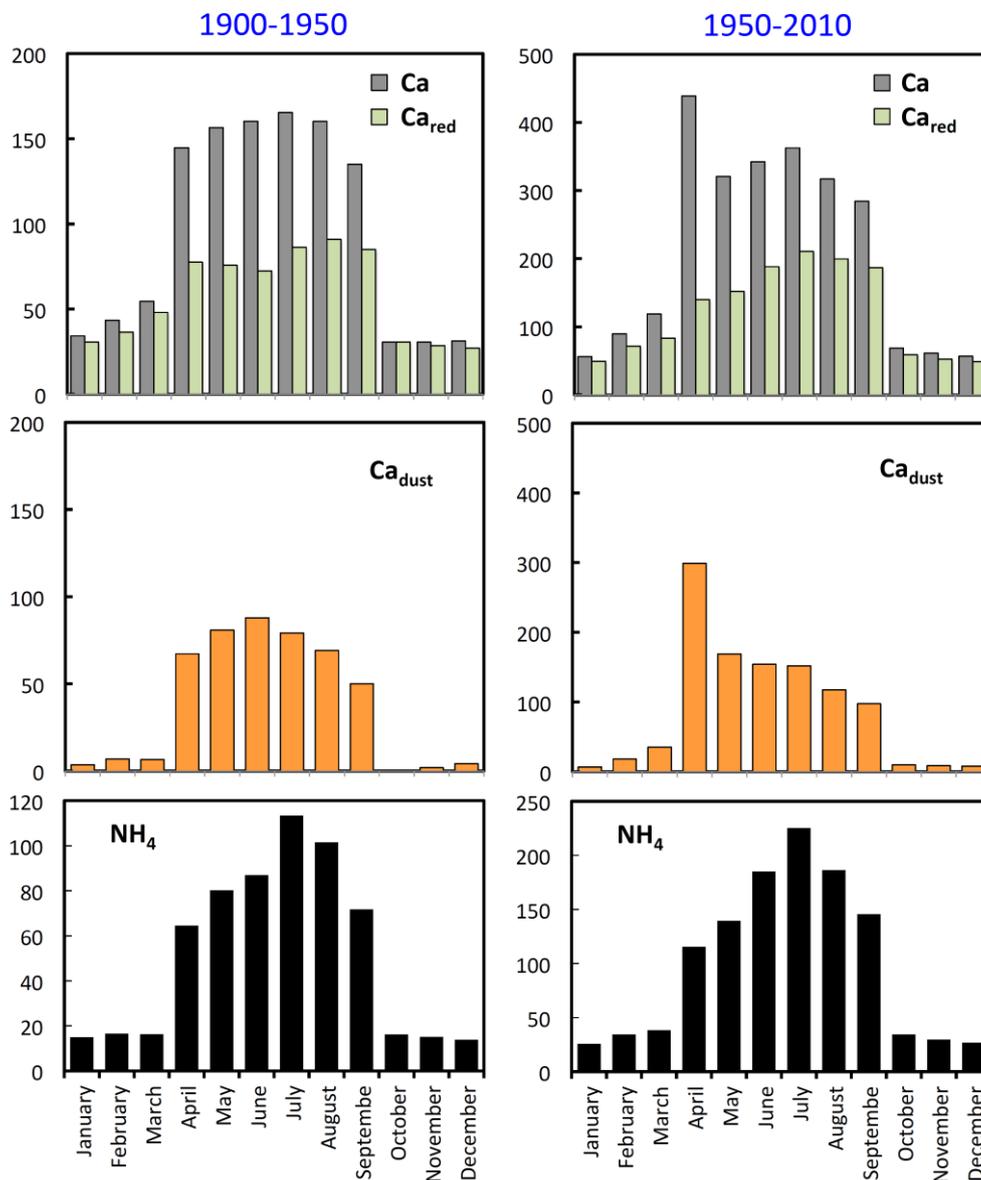
Figure 5: (a): Monthly means of calcium and ammonium (used for determining seasonality as described in the text), over 1900-1950 (left) and 1950-2010 (right). Total calcium concentrations are the grey bars in the top panels while calcium concentrations calculated after the removal of samples are in red. The middle panels refer to calcium concentrations corresponding to the dust fraction (i.e., $[Ca^{2+}]$ - $[Ca^{2+}_{red}]$, orange bars).
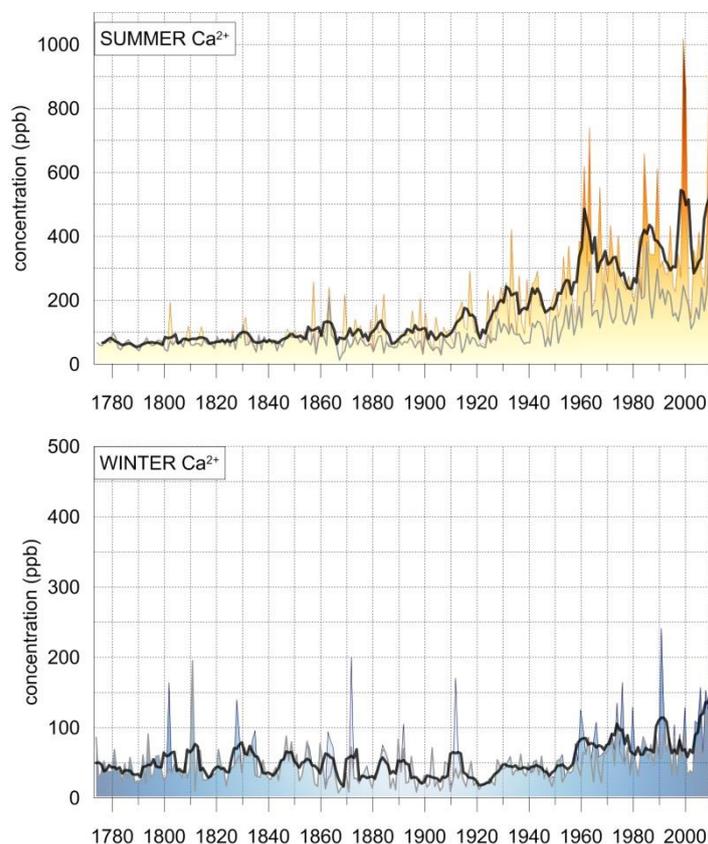
Figure 6: Total and background (grey lines) Ca^{2+} concentrations in Elbrus ice core in summer and winter. 5-year moving averages are shown as black lines.
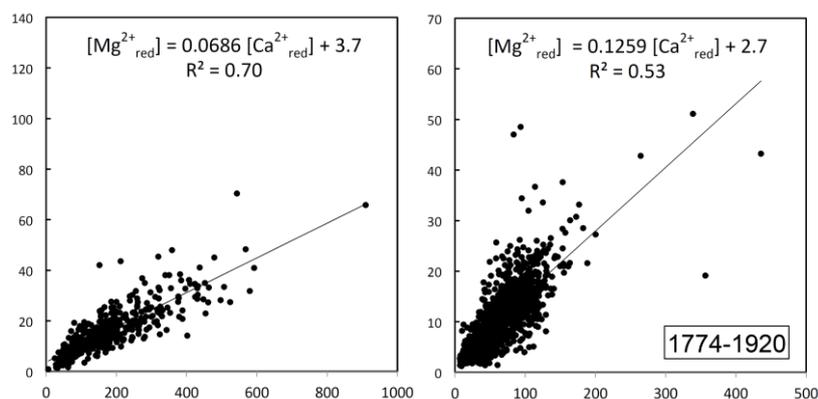
5   **Figure 7: [Mg$^{2+}_{red.}$] versus [Ca$^{2+}_{red.}$] in individual Elbrus ice summer samples (not impacted by dust events) over the recent decades (left) and prior to the 1950 increase in calcium.**
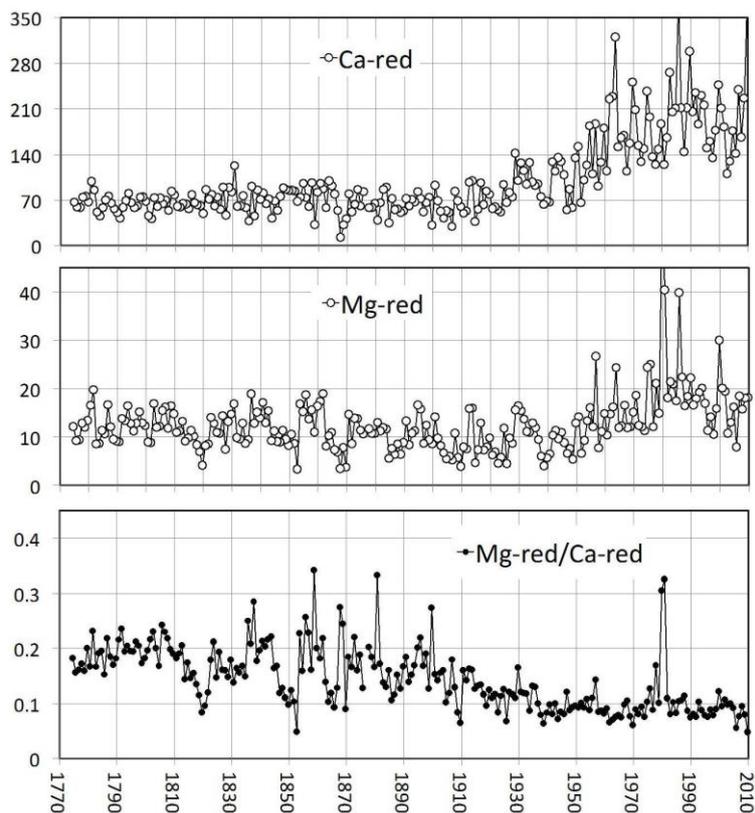
Figure 8: Individual summer means of background levels of Ca^{2+}, Mg^{2+}, and of the [Mg$^{2+}_{red.}$]/[Ca$^{2+}_{red.}$] mass ratio along the Elbrus ice cores.
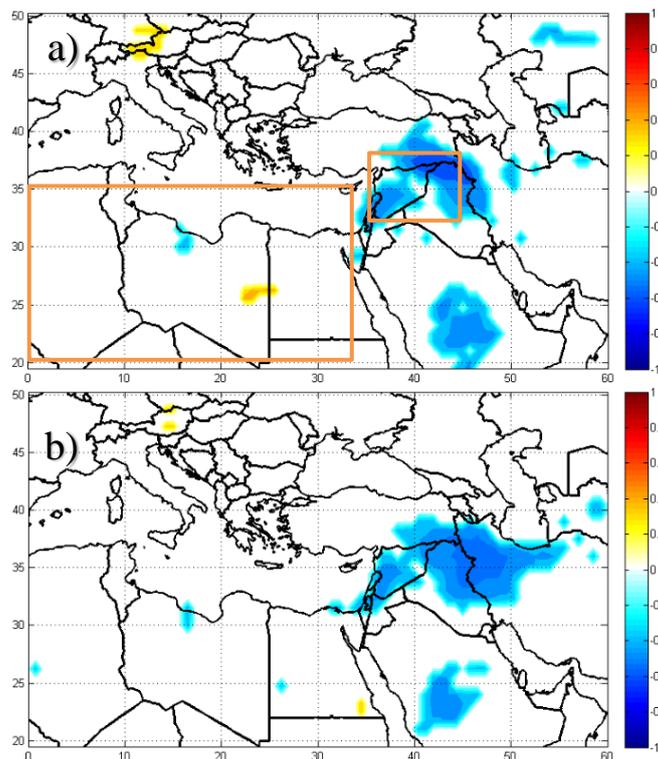
Figure 9: Spatial correlation of Elbrus Ca^{2+} concentrations with soil moisture (a), and precipitation (b) ERA-Interim from 1979 to 2013. North African and Middle Eastern domains are shown by orange boxes.
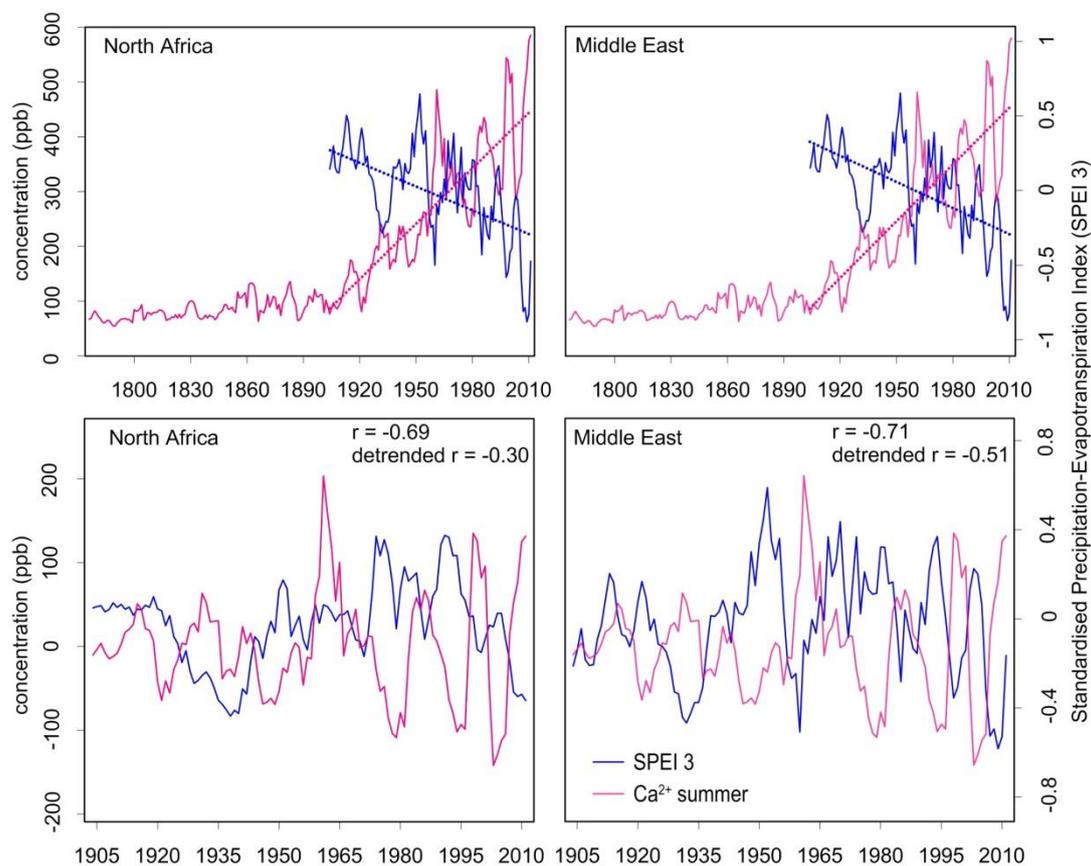
Figure 10: Ca^{2+} and Standardised Precipitation-Evapotranspiration Index (SPEI3) averaged over the regions of (a), (c) North Africa (20-35°N; 0-35°E; and (b), (d) the Middle East (32-37°N; 38-45°E). Outlines of the regions are presented on Figure 9.
5 **Detrended records are shown at the bottom graphs.**
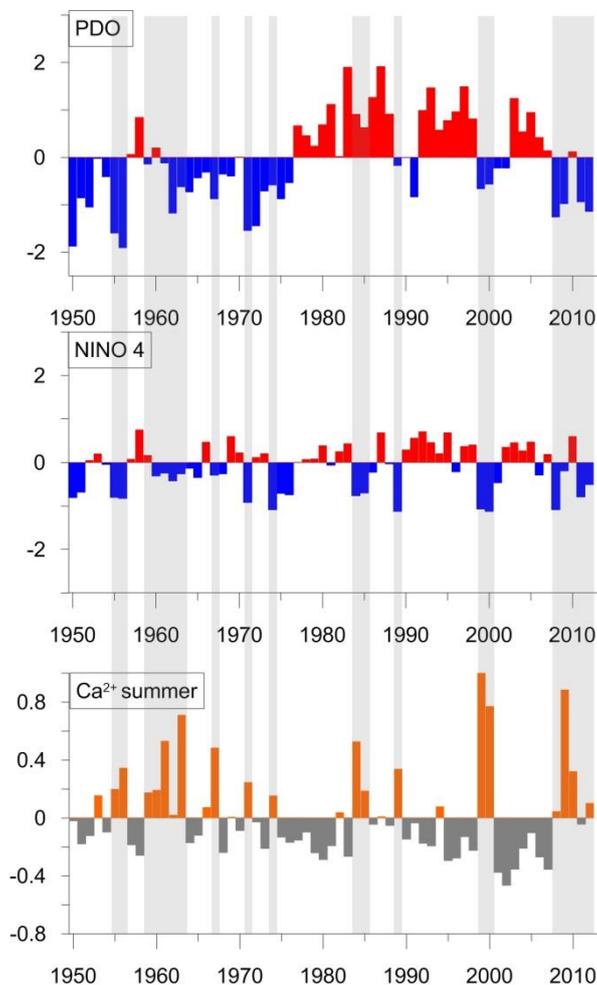
Figure 11: PDO (a) and Niño 4 (b) indices (December-June average), and normalized Ca2+ record (c). Grey shading indicate years when high dust concentrations coincided with negative Niño 4 phases.